

RSC Advances



This is an *Accepted Manuscript*, which has been through the Royal Society of Chemistry peer review process and has been accepted for publication.

Accepted Manuscripts are published online shortly after acceptance, before technical editing, formatting and proof reading. Using this free service, authors can make their results available to the community, in citable form, before we publish the edited article. This *Accepted Manuscript* will be replaced by the edited, formatted and paginated article as soon as this is available.

You can find more information about *Accepted Manuscripts* in the [Information for Authors](#).

Please note that technical editing may introduce minor changes to the text and/or graphics, which may alter content. The journal's standard [Terms & Conditions](#) and the [Ethical guidelines](#) still apply. In no event shall the Royal Society of Chemistry be held responsible for any errors or omissions in this *Accepted Manuscript* or any consequences arising from the use of any information it contains.

**A multi-purpose electrochemical biosensor based on a “green”
homobifunctional cross linker coupled with PAMAM dendrimer
grafted p-MWCNTs as platform: Application to detect
 α 2,3-sialylated glycans and α 2,6-sialylated glycans in human
serum**

*Yazhen Niu¹, Junlin He¹, Yuliang Li, Yilin Zhao, Chunyong Xia, Guolin Yuan, Lei
Zhang, Yuchan Zhang, Chao Yu**

Institute of Life Science and School of Public Health, Chongqing Medical University,
Chongqing 400016, P. R. China

¹Junlin He and Yazhen Niu contributed equally to this work.

*Corresponding author: Prof. Chao Yu,

Email: yuchaom@163.com

Tel: (86) 23-68485589

Fax: (86) 23-68486294

Full address: Box 174#, Institute of Life Sciences, Chongqing Medical University,
No.1 Yixueyuan Road, Yuzhong District, Chongqing 400016, P. R. China.

Abstract

Sialylated glycans are crucial molecular targets for cancer diagnosis and clinical research. α 2, 3-sialylated glycans and α 2, 6-sialylated glycans are predominant sialic acid found in nature. Two kinds of different expression quantity of glycans led to the development of different disease. However, no ideal methods for discriminating α 2,3-sialylated glycans and α 2,6-sialylated glycans. In this work, a multi-purpose biosensor for sensitive detecting of α 2, 3-sialylated glycans and α 2, 6-sialylated glycans is fabricated. For improving the sensitivity of the biosensor, the p-MWCNTs and PAMAM were integrated, owing to the PAMAM with highly branched and abundant amino groups, which provided a large available surface area for linking with other substances. To achieve distinguishable recognition, the *Maackia amurensis lectin* (MAL) and *Sambucus nigra agglutinin* (SNA) as ideal tools for detecting α 2,3-sialylated glycans and α 2, 6-sialylated glycans. In order to further achieve the lectin fixed, PDITC, a kind of green homobifunctional cross linker, was selected. Under optimized detection condition, the linear range of α 2, 3-sialylated glycans is 10 fg mL⁻¹- 50 ng mL⁻¹ with a lower detection limit of 3 fg mL⁻¹, while the linear ranges from 10fg mL⁻¹ to 50 ng mL⁻¹ and a detection limit of 3 fg mL⁻¹ for α 2,6-sialylated glycans are obtained. This work would not only provide a methods for distinguish the detection of α 2,3-sialylated glycans and α 2,6-sialylated glycans but also provide a reference for future clinical testing.

Keywords: α 2,3-sialylated glycans, α 2,6-sialylated glycans, *Maackia amurensis lectin*, *Sambucus nigra agglutinin*, pretreated multi-walled carbon nanotubes, polyamidoamine, 1,4-phenylene diisothiocyana

1. Introduction

Sialic acids (Sia), also known as N-acetylneuraminic acid, is an important component of glycoproteins or glycolipids.¹ Sia have a close relationship in cells adhesion, contact inhibition, cell transformation, metastasis, proliferation and tumor antigenic.² When a cell has been demonstrated pathological changes, the Sia on the cell surface membrane secretion or shedding, thus the content Sia of blood elevated. In the recent studies, the serum sialic acid level of cancer patients was significantly elevated compared with non-malignant.³ All these investigations indicated that the expression level of glycans can be used as a target or clinical biomarker for diagnosis of various cancers.⁴ α 2, 3-sialylated glycans and α 2, 6-sialylated glycans are predominant sialic acid found in nature.^{5, 6} Therefore, α 2, 3-sialylated glycans and α 2,6-sialylated glycans are crucial molecular targets for cancer diagnosis. Two kinds of different expression quantity of glycans led to the development of different disease. For example, the expression of α 2, 3-sialylated glycans quantity increases in the patients with gastric cancer, prostate cancer⁷ and so on, the α 2,6-sialylated glycans high expression was found in liver cancer and colon cancer.⁸ However, no methods were used to discrimination α 2, 3-sialylated glycans and α 2, 6-sialylated glycans. Therefore, a simple, sensitive and discrimination of α 2, 3-sialylated glycans and α 2,6-sialylated glycans method is required.

The remarkable chemical diversity of sialylated glycans (α 2, 3, α 2, 6) resulted in multiple enzymatic mechanisms,^{1, 9} which can be recognized by the specific lectin. Certain Sia-binding lectins have been proven to be a powerful tool for directly Sia-specific glycoconjugates.¹⁰ For example, *Limax flavus agglutinin* and *wheat germ agglutinin* were used to detect sialylated glycoconjugates.¹⁰⁻¹² *Sambucus nigra agglutinin* (SNA) is an ideal tool for recognizing α 2,6-sialylated glycans and *Maackia amurensis lectin* (MAL) an ideal tool for recognizing α 2,3-sialylated glycans.¹³ Accurate analysis of biomarker molecules for early detection, diagnosis and treatment of cancer are essential.¹⁴ Electrochemical biosensor based on various types of nanomaterials is fast, simple and high sensitivity, which may provide an alternative

way for sialic acids.

For electrochemical biosensors, considerable efforts have been devoted to amplify and immobilizing bio-components.¹⁵ It has been found that the multiwalled carbon nanotubes (MWCNTs) modified electrodes had a better electrochemical behavior than those used the single-walled carbon-nanotubes (SWCNTs).¹⁶ In addition, when chemical modification upon the surface of MWCNTs, the outer cylinder acts as a protective sheath so that the electronic properties of the inner tube are protected.¹⁷ But the MWCNTs have a poor biocompatibility and dispersion. In this study we used carboxyl-functionalized multiwalled carbon nanotubes (p-MWCNTs), which would overcome the poor biocompatibility and dispersion. Compared with non-functional MWCNTs, p-MWCNTs possess carboxyl groups and its sizes are shorter.¹⁶ Despite the carboxyl-functionalized can improve the dispersion of MWCNTs in part, they have a certain limits in the practical application. So the PAMAM was used to further improve the dispersion.

Polyamidoamine (PAMAM) dendrimers are highly branched and monodispersed macromolecules that have a well-defined three-dimensional and globular structure.¹⁷ The number of peripheral amine groups of PAMAM (G5.0) reaches 64, being very suitable for combined with p-MWCNTs. Besides, when PAMAM integrated with the p-MWCNTs, the stability of the biosensor was improved. The massive amine may enhance the immobilization of 1, 4-phenylene diisothiocyanate (PDITC). PDITC is a kind of green homobifunctional cross linker that was chosen due to its stability, flexibility and lower toxicity.¹⁸ PDITC was used to immobilize the SNA and MAL. And the PDITC can substitute the glutaraldehyde owing to the conductive of PDITC better than glutaraldehyde.¹⁹

In this report, we reported an ultrasensitive and multi-purpose biosensor for the detection of $\alpha 2, 3$ -sialylation and $\alpha 2, 6$ -sialylation for the first time. The p-MWCNTs have a large surface area and possess certain carboxyl groups, which were successfully conjugated with PAMAM. And PDITC as a homobifunctional cross agent to link between PAMAM and lectin. The multi-purpose biosensor exhibited excellent electrochemical response to the specifically detection of $\alpha 2, 6$ -sialylation and

α 2,3-sialylated glycans.

2. Experimental

2.1 Material and reagents

Neu5Aca(2-6)Gal β MP Glycoside and Neu5Aca(2-3)Gal β MP Glycoside was purchased from Tokyo Chemical Industry (Japan, www.TCIchemicals.com, 90.0%). *Sambucus nigra agglutinin* (SNA) and *Maackia amurensis lectin* (MAL) was purchased from Vector Labs (www.vectorlabs.com). 1,4-phenylene diisothiocyanate ($C_6H_4(NCS)_2$), Polyamidoamine PAMAM dendrimer, Bovine serum albumin (BSA, 96-99%), N-Hydroxysuccinimide (NHS) and N-(3Dimethylaminopropyl)-N-ethylcarbodiimide hydrochloride (EDC) was purchased from Sigma (St. Louis, USA, www.sigmaaldrich.com). Dopamine (DA), Ascorbic acid (AA), L-cysteine and glucose were obtained from Aladdin (China, www.aladdin-e.com). The other chemicals were of analytical and all solutions were prepared in ultrapure water.

2.2 Apparatus and measurements

The morphology of the pretreated multiwalled carbon nanotubes (p-MWCNTs) and the pretreated multiwalled carbon nanotubes-polyamidoamine dendrimer (p-MWCNTs-PAMAM) microspheres were characterized by transmission electron microscopy (TEM, Hitachi-7500) and scanning electron microscopy (SEM, Hitachi-7500518). Atomic force microscope (AFM) images were obtained with a Bruker Dimension Icon microscope (USA). Differential Scanning Calorimeter (DSC) was performed using STA449 F3 Jupiter. In this electrochemical experiments, electrochemical impedance spectroscopy (EIS), differential pulse voltammetry (DPV) and cyclic voltammetry (CV) were carried out utilizing an electrochemical workstation (CHI660E) and a three-electrode system (Shanghai Chenhua Apparatus

Corporation, China) composed of a glassy carbon electrode (GCE, 4 mm in diameter) as a working electrode, platinum serving as the counter electrode, and a saturated calomel electrode (SCE) serving as the reference electrode. 5 mM $K_3[Fe(CN)_6]/K_4[Fe(CN)_6]$ (1:1) and 0.1 M KCl were used to all of the electrochemical measurements.

2.3 Preparation of pretreated multi-walled carbon nanotubes

The methods of pretreated multi-walled carbon nanotubes were according to previous reports^{20, 21} with slight changes. Briefly, 10 mg of MWCNTs (in solid form) were refluxed in a H_2SO_4 - HNO_3 mixture (3:2 by volume) for 24 h and dried under vacuum until a white solid residue, and then use distilled water wash for several times until the pH of the solution reached 7.0. The resultant was dried in oven. The carboxyl groups functionalized MWCNTs were obtained.

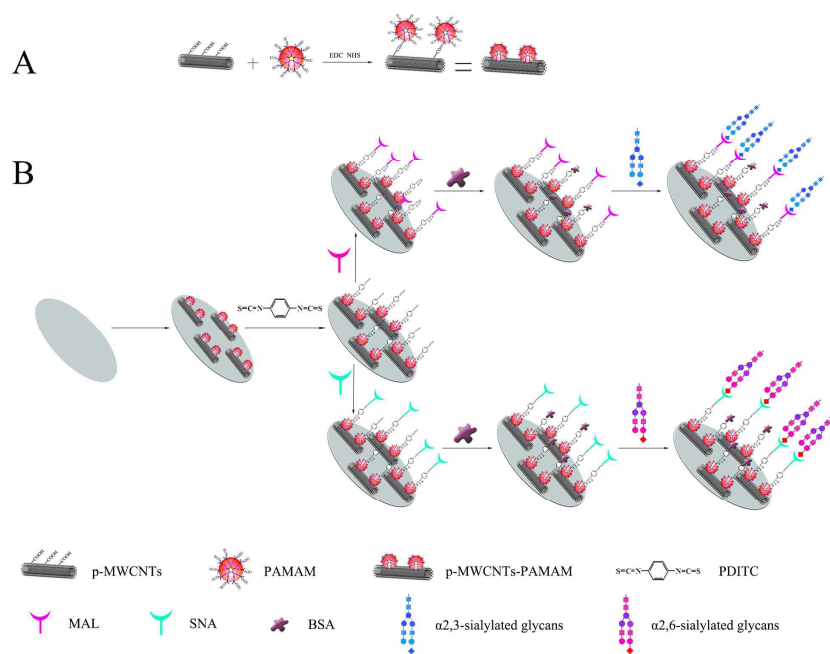
2.4 Preparation of the p-MWCNTs-PAMAM complex

The p-MWCNTs-PAMAM nanocomposite was prepared according to the literature with slight modifications.²² 2 mg of MWCNTs was added to ultrapure water under ultrasonication for 2 h. The nanocomposite was subsequently mixed with 50 μ L of NHS (50 mg mL^{-1}) and 50 μ L of EDC (50 mg mL^{-1}) with stirring 30 min. Then 50 μ L PAMAM was added into the resulting mixture and stirred for 5 h. The p-MWCNTs-PAMAM was obtained and the prepared process was shown in Scheme 1A.

2.5 Fabrication of the biosensor

The biosensor was prepared following the steps outlined in Scheme. 1B. Prior to use, the glassy carbon electrode (GCE) was polished carefully with Al_2O_3 powder of

0.3 and 0.05 μm to like mirror surface. Then, 6 μL of as-prepared p-MWCNTs-PAMAM was dropped onto the electrode surface and dried at room temperature. Next, 6 μL of PDITC solution was added to the p-MWCNTs-PAMAM/GCE and incubated for 1 h at room temperature. After washing with distilled water, 6 μL of SNA and MAL were coated onto the electrode surface and incubated for 2 h to yield a MAL/PDITC/p-MWCNTs-PAMAM/GCE, respectively. 6 μL of a 1 wt% BSA was added to the modified electrode for 1 h, which in order to block the nonspecific binding sites. Subsequently, 6 μL of a standard α 2,6-sialic acid solution and standard α 2,3-sialic acid solution dropped onto electrode surface and left standing for 2 h. After each step, the modified electrode was cleaned thoroughly with ultrapure water. The biosensor for the determination of α 2,3-sialylated glycans and α 2,6-sialylated glycans were accomplished (Scheme 1B).



Scheme 1. Schematic representation of the electrochemical biosensor.

3. Results and discussion

3.1 Characterization of prepared material

Fig. 1 shows the TEM images of p-MWCNTs and p-MWCNTs-PAMAM. Fig. 1A shows the TEM image of the p-MWCNTs, revealing that the tubular structure of p-MWCNTs. It can be seen that a lot of scattered and small black dots (PAMAM) connect with p-MWCNTs (Fig 1B and Fig 1C). The length of p-MWCNTs is approximately 0.5 μm (Fig 1C), which is shorter than the length of normal multi-walled carbon nanotubes (5-20 μm).²³ This finding suggests that the p-MWCNTs-PAMAM was successfully prepared. To obtain more evidence to confirm the p-MWCNTs-PAMAM was successfully prepared, differential scanning calorimeter (DSC) and UV-Vis spectroscopy further confirmed the formation of p-MWCNTs-PAMAM. The fig S2 shows the p-MWCNTs no significant change in the value of DSC. The PAMAM have an exothermic peak at 290-300 $^{\circ}\text{C}$. When p-MWCNTs-PAMAM was prepared, the exothermic peak of PAMAM disappears. Meanwhile, as can be seen in fig 1D, the pure p-MWCNTs solution displayed a characteristic band at 300 nm (red line).^{24, 25} For the PAMAM, the characteristic absorption at 280 nm (blue line). Typical absorption peaks of an aromatic system at 250-300 nm, which is similar to the polycyclic aromatic hydrocarbons.^{26, 27} After p-MWCNTs connected with PAMAM, the absorption band at 420 nm (black line). All of these results indicated that the successful synthesis of the nanocomposites. When the p-MWCNTs solution and the p-MWCNTs-PAMAM solution stored 7 days, the p-MWCNTs solution created an inhomogeneous mixture and the p-MWCNTs-PAMAM solution was homogeneous in Fig 1E and Fig 1F. Obviously, the stability of the solution was improved when PAMAM combined with p-MWCNTs.

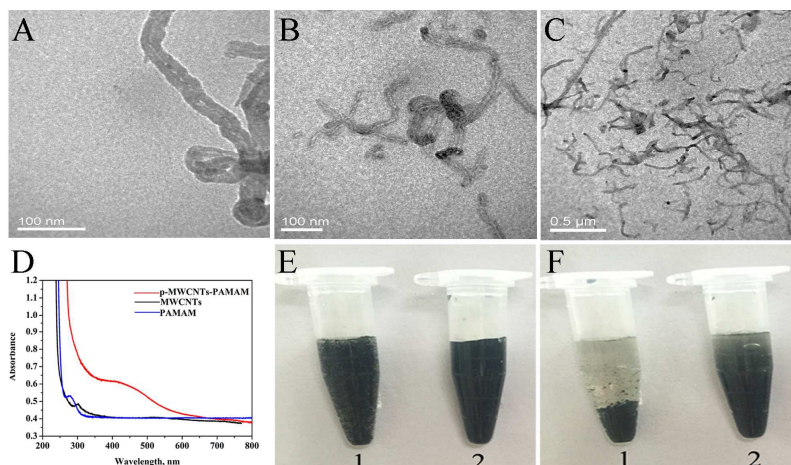


Fig. 1. TEM image of p-MWCNTs (A) and p-MWCNTs-PAMAM (B and C), The UV-vis (D) spectroscopy of p-MWCNTs (black), PAMAM (blue) and p-MWCNTs-PAMAM (red), the photographs (E and F) p-MWCNTs solution (E1,F1) and p-MWCNTs-PAMAM (E2,F2).

To obtain more evidence to confirm the successful immobilization of PDITC and MAL on the nanocomposite film surface, atomic force microscopy (AFM) was used to investigate the bioconjugation process. Fig 2 shows the three dimensional images of p-MWCNTs-PAMAM (A), PDITC/p-MWCNTs-PAMAM (B) and MAL/PDITC/p-MWCNTs-PAMAM (C). The greatest peak height of the p-MWCNTs-PAMAM was 21.92 nm (Fig 2A). The average roughness (Ra) was 3.71 nm. After the immobilization of PDITC on the p-MWCNTs-PAMAM, the peak height was approximately 16.40 nm and the Ra was 2.73 nm, due to the PDITC aggregates filling the gaps on the nanocomposite (Fig 2B). When the MAL linked with PDITC, the greatest peak height was 11.40 nm and Ra was 1.62 nm. The surface roughness MAL/PDITC/p-MWCNTs-PAMAM of become smooth further compared with PDITC/p-MWCNTs-PAMAM (Fig 2C), due to MAL covered the gaps in the electrode surface.²⁸ All of these results suggested that the successful fabrication of the biosensor. The roughness of SNA/PDITC/p-MWCNTs-PAMAM biosensor was similar with MAL/PDITC/p-MWCNTs-PAMAM biosensor.

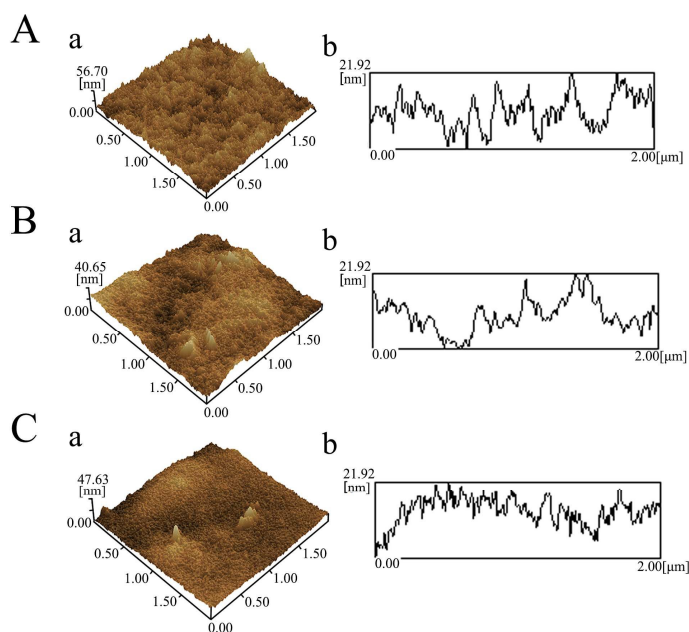


Fig 2. AFM AFM images of (a) three dimensional and (b) cross-sectional graphs of (A) p-MWCNTs-PAMAM, (B) PDITC/p-MWCNTs-PAMAM and (C) MAL/PDITC/p-MWCNTs-PAMAM

3.2 Electrochemical characterization of the stepwise-modified electrode

Electrochemical impedance spectroscopy (EIS) is an effective method for the electron-transfer resistance at an electrode surface and studying the interface properties of surface-modified electrodes.²⁹ The impedance spectra include a semicircle portion and a linear portion. The linear portion at lower frequencies corresponds to the diffusion-limited process. The semicircle portion at higher frequencies represents the electron transfer limited process. The semicircle diameter equals the electron transfer resistance (R_{et}).²⁹ As shown in Fig 3B, the bare GCE presents a small semicircle at high frequency (curve a) of R_{et} value of 307.6 Ω . After the electrode was modified with p-MWCNTs-PAMAM, the resistance was much less than the bare GCE (curve b, $R_{et} = 182.2 \Omega$), suggesting that the p-MWCNTs-PAMAM in favor of interfacial and electron transfer. The resistance increased after incubation with PDITC (curve c, 372.0 Ω), which indicating PDITC was linked with

p-MWCNTs-PAMAM. The resistance continued to increase after incubation with MAL (curve d, 507.7 Ω), indicating that MAL was immobilized on the modified electrode successfully, due to MAL blocking electron transfer. After BSA blocked electrode the peak currents continued to decrease because electron hindrance of BSA, the R_{et} was enlarged (curve e, 909.9 Ω). Subsequently, the R_{et} of curve f increased (1032.0 Ω) because the Neu5Aca(2-3)Gal β MP Glycoside was captured by MAL. The inset in Figure 3B (top right corner) is the equivalent circuit used to fit the impedance spectra. This circuit includes the constant phase element CPE related to the double layer capacitance, C_{dl} , the electrolyte solution, R_s , the Warburg impedance, Z_w , which is a cause of the diffusion of the redox probe ions to the electrode interface from the bulk of the electrolyte, and the resistance of the electron transfer, R_{et} . The dates obtained after fitting the resistance spectra are recorded in Table 1. The data of the CV are in agreement with the result from EIS, suggesting the successful fabrication of the biosensor.

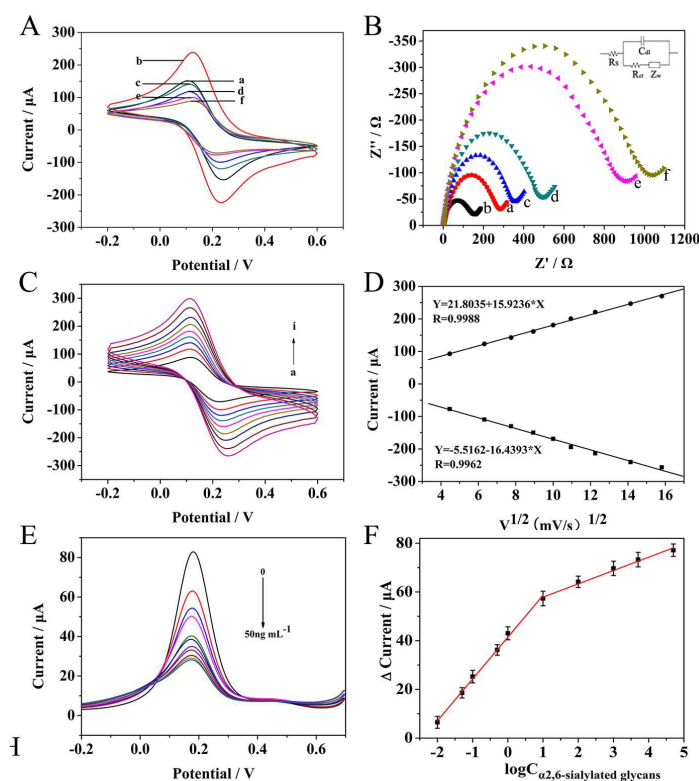


Fig 3. Typical CV (A) and (B) studies of K₃[Fe(CN)₆]/K₄[Fe(CN)₆] (5mM) for (a) a bare electrode, (b) p-MWCNTs-PAMAM/GCE, (c) PDITC/p-MWCNTs-PAMAM/GCE, (d)

MAL/PDITC/p-MWCNTs-PAMAM/GCE, (e) blocking with 1%BSA and (f) specific recognition with 5 ng ml⁻¹ Neu5Aca(2-6)Gal β MP glycoside; Cyclic voltammograms of the electrochemical biosensor at different scan rates ranging from 20 to 250 mV s⁻¹ in [Fe(CN)₆]^{3-/4-} (1:1) and 0.1 M KCl; (D) The liner relation of current versus the square root of the scan rates; (E) DPV responses of the proposed biosensor after incubation with different concentrations of Neu5Aca(2-6)Gal β MP Glycoside; (F) Calibration curve of the biosensor toward different concentration of Neu5Aca(2-6)Gal β MP Glycoside (n=5).

Table 1

Simulation parameters of the equivalent circuit components.

Electrode	R_s (Ω cm ²)	R_{et} (Ω cm ²)	C_{dl} (μ F cm ²)	n	$10^3 Z_w$ (Ω cm ²)
GCE	12.22	21.36	72.02	0.84	0.19
p-MWCNTs-PAMAM/GCE	5.08	10.71	23.40	0.84	0.18
PDITC/p-MWCNTs-PAMAM/GCE	5.95	26.81	57.32	0.86	0.64
MAL/PDITC/p-MWCNTs-PAMAM/GCE	4.86	33.80	10.82	0.89	0.39
blocking with 1%BSA	5.98	75.53	27.12	0.86	1.50
50 ng ml ⁻¹ Neu5Aca(2-3)Gal β MP glycoside	6.69	84.91	34.90	0.84	0.51

The influence of the potential scan rate on the peak current response about PDITC/p-MWCNTs-PAMAM electrode was investigated. The CV of PDITC/p-MWCNTs-PAMAM in 5 mM of K₃[Fe(CN)₆]/K₄[Fe(CN)₆] at different scan rates were shown in Fig 3C. The redox peaks current increased gradually with the increasing of scan rate in the range of 20-250 mV s⁻¹. Fig 3D show a good liner relationship between the peak current and the square root of scan rate. This result indicates that the redox reaction on the electrode surface is a diffusion-controlled process, which was consistent with previously reported.³⁰ According to the Randles-Sevcik equation^{31,32} $I = 2.69 \times 10^5 A \times D^{1/2} n^{3/2} \nu^{1/2} C$, in which n is the number of electrons transferred in the redox reaction ($n = 1$), A is the electrode area, C is the concentration of the reactant (at 25 °C, $D = 6.70 \times 10^{-6}$ cm² s⁻¹), (5 mM K₃[Fe(CN)₆]/K₄[Fe(CN)₆]), D is the diffusion coefficient, I refers to the redox peak current and ν is the scan rate of the CV measurement, the surface area of the PDITC/p-MWCNTs-PAMAM modified electrode was calculated to be 30.84 mm².

3.3 Optimization of experimental conditions

The electrochemical performance of the biosensor may be influenced by the experiment conditions. Therefore, the volume of p-MWCNTs-PAMAM hybrid nanocomposite, the incubation time of PDITC, the concentration of MAL and SNA, the incubation time of MAL, incubation time of SNA and the length of recognition time were investigated.

As shown in Fig. 4A, the current response increased rapidly with increasing PAMAM volumes from 20 μL to 50 μL . With increase the volume of PAMAM led to decrease the current change, possibly because the excess PAMAM fail to conjugate with MWCNTs. Thus, 50 μL of the PAMAM was used as the optimal condition.

The volume of p-MWCNTs-PAMAM was investigated to provide a good platform for incubation with PDITC. The volume of p-MWCNTs-PAMAM was test in the range from 2 μL to 10 μL . The current change increased until a volume of 6 μL , then remained stable (Fig. 4B). Therefore, 6 μL was determined to be the optimal volume of p-MWCNTs-PAMAM.

The time of incubation PDITC is a critical factor for the process of the biosensor. PDITC plays a key role in providing functional group for MAL immobilization. As shown in Fig. 4C, the current change increased sharply from 30 min to 60 min and reached a maximum at 60 min. Further increase in incubation time the current was no significant change. Therefore, 60 min was selected as the optimal incubation time for this experiment.

To optimize the reaction time, the assembly time of analysis on SNA were investigated (Fig. 4D). A period of time is required for the lectin to bind the sialylated glycans and form a complex. Gradually increasing the reaction time led to outstanding decrease of signal, which implies that SNA were immobilized on binding sites and hindered electron transfer. In our work, the SNA observed response from 30 min to 180 min, in which the current change initially increases then stable and the highest peak at 150 min. Thus, 150 min was selected as the best incubation time of SNA in this work.

Besides, the concentration of SNA is also an important factor in the experiment. When the number of SNA that fixed on electrode surface was maximized, the biosensor has high sensitivity. The concentration range from 0.5 mg mL⁻¹ to 2.5 mg mL⁻¹ was investigated (Fig. 4E). The changes of current increased until 2.0 mg mL⁻¹, then remained stable. Therefore, 2.0 mg mL⁻¹ was selected as the optimal concentration for the experiment.

The time of incubation of Neu5Aca(2-6)Gal β MP Glycoside is notably important parameter due to glycoside was recognized by SNA and required time to form a complex. To explore the effect of the incubation time on amperometric response, incubated time of the fabricated biosensor from 60 to 180 min was chosen (Fig. 4F). With time increased, the more glycoside was captured by lectin and the current change was enlarged. With the incubation time from 60 min to 120 min, the current change gradually increased, then reached stable. It reveals that the amount of Neu5Aca(2-6)Gal β MP Glycoside captured on the sensor surface and reached maximum. Therefore, the optimal incubation time of SNA was 150 min.

The MAL experimental conditions were found to give best results (Fig. S3A-C): (d) incubation time of 2 h of the MAL; (e) concentration of 2.0 mg mL⁻¹ of the MAL; (f) recognition time 2 h of the α2,3-sialylated glycans.

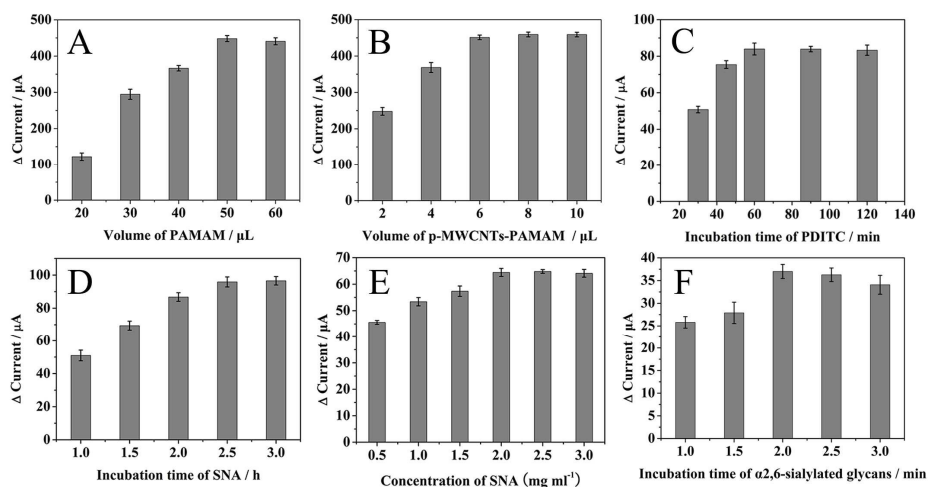


Fig 4. Effects of (A) volume of PAMAM, (B) volume of p-MWCNTs-PAMAM, (C) incubation

time of PDITC, incubation time of SNA (D), concentration of SNA (E), recognition time of α 2,6-sialylated glycans (F).

3.4 Performance of the biosensor

The calibration plot for the detection of Neu5Aca(2-3)Gal β MP Glycoside and Neu5Aca(2-6)Gal β MP Glycoside were determined under the optimal experimental conditions. As shown in Fig. 3E and Fig. 3F, the prepared electrochemical biosensor was used to detect Neu5Aca(2-3)Gal β MP Glycoside and Neu5Aca(2-6)Gal β MP Glycoside by DPV. With the increased concentration of glycoside, the formed Glycan-lectin complexes increased and the spread of the redox probe was gradually blocked. This finding indicates that the change of the current response is related to the amount of glycoside captured on the electrode surface. Therefore, the peak current response decreased as the concentrations of Neu5Aca(2-6)Gal β MP Glycoside increased. The calibration plot has a good linear relationship in the range of 10 fg mL⁻¹ to 50 ng mL⁻¹ with a detection limit of 3 fg mL⁻¹ (S/N = 3). As shown in Fig. S2, for accuracy of the detection, the equation of the calibration plot was separated into two parts. For values below 10 pg mL⁻¹, the equation used was $\Delta\text{Current} (\mu\text{A}) = 65.71 + 18.53 \log C$, $R^2 = 0.997$. Over 10 pg mL⁻¹, the equation used was $\Delta\text{Current} (\mu\text{A}) = 79.72 + 3.34 \log C$, $R^2 = 0.986$. As shown in Figure 3F, Below values of 10 pg mL⁻¹, the equation used was $\Delta\text{Current} (\mu\text{A}) = 59.00 + 20.95 \log C$, $R^2 = 0.988$. Over 10 pg mL⁻¹, the equation was used: $\Delta\text{Current} (\mu\text{A}) = 79.66 + 3.39 \log C$, $R^2 = 0.980$. Therefore, novel and specific biosensor was designed to sensitively detect the Neu5Aca(2-3)Gal β MP Glycoside and Neu5Aca(2-6)Gal β MP Glycoside within the analytical concentration range.

3.5 Selectivity, stability and reproducibility of the electrochemical biosensor

To evaluate the selectivity of the electrochemical biosensor, we explored the effect of other molecules on the system including Neu5Aca(2-3)Gal β MP Glycoside,

ascorbic acid (AA), L-cysteine (L-cys), glucose, uric acid and dopamine (DA). These studies confirmed that the change of current was due to the specific recognition between glycoside and lectin (Figure 5A). The current change caused by other molecules was less than 10%, suggesting that the fabricated biosensor exhibited good selectivity and the biosensor can distinguish detection α 2,3-sialylated glycans and α 2,6-sialylated glycans.

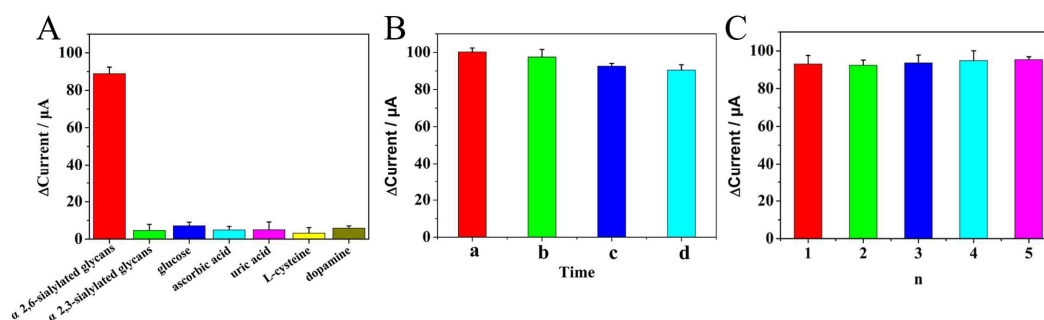


Fig. 5A α 2,6-sialylated glycans (50 ng mL^{-1}), α 2,3-sialylated glycans (500 ng mL^{-1}), glucose (500 ng mL^{-1}), ascorbic acid (500 ng mL^{-1}), uric acid (500 ng mL^{-1}), L-cysteine (500 ng mL^{-1}) and dopamine (500 ng mL^{-1}); The stability of the electrochemical biosensor after 0 days (a), 7 days (b), 14 days (c) and 21 days (d) (5C); The reproducibility of five different electrodes modified with 50 ng mL^{-1} α 2,6-sialylated glycans (5D).

The MAL/PDITC/p-MWCNTs-PAMAM/GCE modified electrode was stored at $4 \text{ }^\circ\text{C}$. The changed current was retained at 95.21%, 91.92% and 89.42% compared with the original current after 7, 14 and 21 days, respectively (Figure 5B). Possible reasons for this observation include the following: (1) p-MWCNTs-PAMAM has a good biocompatibility and stability and (2) MAL has strong specific recognition ability.

The reproducibility of the electrochemical biosensor was evaluated. The intra-assay precision of the biosensor was estimated by analyzing five prepared electrodes for the detection of Neu5Ac α (2-6)Gal β . The relative standard deviations (RSD) of the measurements for the five electrodes was 3.31% at a Neu5Ac α (2-6)Gal β MP glycoside concentration of 50 ng mL^{-1} , indicating acceptable precision and good

reproducibility (Figure 5C).

3.6 Application Analysis in Human Serum Samples

To examine the applicability of the present electrochemical biosensor to real samples, the determination of Neu5Aca(2-6) Gal β MP glycoside in human serum was performed using DPV analysis. The diluted human serum samples spiked with 1 ng mL⁻¹, 5 ng mL⁻¹ and 40 ng mL⁻¹ Neu5Aca(2-6) Gal β MP glycoside, were applied to the electrochemical biosensor (Table 2). The application analysis of the Neu5Aca(2-3) Gal β MP glycoside was shown in supplementary materials (Table S1).

Tab 2. Recovery of serum samples for the electrochemical biosensor using Amperometric i-t curve analysis (n = 3).

Samples	C _{analyte}	Added	Found ^b	Recovery	RSD (%)
Sample-1	NT	0.5 pg mL ⁻¹	0.51 pg mL ⁻¹	101.72	4.29
Sample-2	NT	5 ng mL ⁻¹	5.21 ng mL ⁻¹	104.25	3.27
Sample-3	NT	40 ng mL ⁻¹	39.32 ng mL ⁻¹	98.32	1.64

4. Conclusions

We report an ultrasensitive and specific electrochemical biosensor based on PDITC cross linked with p-MWCNTs-PAMAM to distinguish detection of α 2,3-sialylated glycans and α 2,6-sialylated glycans in human serum and detection of α 2,3-sialylated glycans for the first time. The developed electrochemical biosensor has a high specificity and a broad liner range with a low detection limit, indicating resilience to endogenous interferences in human serum. The biosensor also has good reproducibility and high sensitivity, which would be used as rapid analytical tool for diagnostic and clinical research. The p-MWCNTs-PAMAM biosensor may find wide applications in the routine detection of other proteins or glycans, which will require the use of other affinity binding pairs.

Acknowledgments

This study was supported financially by the National Natural Science Foundation of China (81370403, 21205146).

References:

1. S. Kim, D. B. Oh, H. A. Kang and O. Kwon, *Applied microbiology and biotechnology*, 2011, 91, 1-15.
2. A. Varki, *Nature*, 2007, 446, 1023-1029.
3. R. J. Winzler, *Methods of biochemical analysis*, 1955, 2, 279-311.
4. Y. K. Matsuno, T. Saito, M. Gotoh, H. Narimatsu and A. Kameyama, *Analytical chemistry*, 2009, 81, 3816-3823.
5. D. B. Werz, R. Ranzinger, S. Herget, A. Adibekian, C. W. von der Lieth and P. H. Seeberger, *ACS chemical biology*, 2007, 2, 685-691.
6. R. J. Fair, H. S. Hahm and P. H. Seeberger, *Chemical communications*, 2015, 51, 6183-6185.
7. C. Ohyama, M. Hosono, K. Nitta, M. Oh-eda, K. Yoshikawa, T. Habuchi, Y. Arai and M. Fukuda, *Glycobiology*, 2004, 14, 671-679.
8. T. Sata, J. Roth, C. Zuber, B. Stamm and P. U. Heitz, *The American journal of pathology*, 1991, 139, 1435-1448.
9. T. J. Boltje, T. Buskas and G. J. Boons, *Nature chemistry*, 2009, 1, 611-622.
10. L. Gao, J. He, W. Xu, J. Zhang, J. Hui, Y. Guo, W. Li and C. Yu, *Biosensors & bioelectronics*, 2014, 62, 79-83.
11. J. J. Park, J. Y. Yi, Y. B. Jin, Y. J. Lee, J. S. Lee, Y. S. Lee, Y. G. Ko and M. Lee, *Biochemical pharmacology*, 2012, 83, 849-857.
12. N. Shibuya, I. J. Goldstein, W. F. Broekaert, M. Nsimba-Lubaki, B. Peeters and W. J. Peumans, *Archives of biochemistry and biophysics*, 1987, 254, 1-8.
13. C. Geisler and D. L. Jarvis, *Glycobiology*, 2011, 21, 988-993.
14. X. Liu, Q. Dai, L. Austin, J. Coutts, G. Knowles, J. Zou, H. Chen and Q. Huo, *Journal of the American Chemical Society*, 2008, 130, 2780-2782.
15. G. Yuan, C. Yu, C. Xia, L. Gao, W. Xu, W. Li and J. He, *Biosensors & bioelectronics*, 2015, 72, 237-246.
16. Y. Liang, H. Wang, P. Diao, W. Chang, G. Hong, Y. Li, M. Gong, L. Xie, J. Zhou, J. Wang, T. Z. Regier, F. Wei and H. Dai, *Journal of the American Chemical Society*, 2012, 134, 15849-15857.
17. D. M. Kim, M. A. Rahman, M. H. Do, C. Ban and Y. B. Shim, *Biosensors & bioelectronics*, 2010, 25, 1781-1788.
18. R. Elshafey, C. Tlili, A. Abulrob, A. C. Tavares and M. Zourob, *Biosensors & bioelectronics*, 2013, 39, 220-225.
19. Y. Zhao, J. He, G. Yuan, C. Xia, Y. Li and C. Yu, *RSC Adv.*, 2015, 5, 88392-88400.
20. C. Zhu, S. Guo and S. Dong, *Advanced materials*, 2012, 24, 2326-2331.
21. W. Xu, J. He, L. Gao, J. Zhang and C. Yu, *Microchimica Acta*, 2015, 182, 2115-2122.
22. J. Zhang, J. He, W. Xu, L. Gao, Y. Guo, W. Li and C. Yu, *Electrochimica Acta*, 2015, 156, 45-52.
23. W. Qiu, H. Xu, S. Takalkar, A. S. Gurung, B. Liu, Y. Zheng, Z. Guo, M. Baloda, K. Baryeh and G. Liu, *Biosensors & bioelectronics*, 2015, 64,

- 367-372.
24. X. Zhang, W. Lu, J. Shen, Y. Jiang, E. Han, X. Dong and J. Huang, *Biosensors & bioelectronics*, 2015, 74, 291-298.
 25. Y. Yao, X. Bai and K.-K. Shiu, *Nanomaterials*, 2012, 2, 428-444.
 26. Q. Gao, J. Han and Z. Ma, *Biosensors & bioelectronics*, 2013, 49, 323-328.
 27. S. Y. Xie, R. B. Huang and L. S. Zheng, *Journal of chromatography. A*, 1999, 864, 173-177.
 28. Y. Li, L. Fang, P. Cheng, J. Deng, L. Jiang, H. Huang and J. Zheng, *Biosensors & bioelectronics*, 2013, 49, 485-491.
 29. Y. Li, J. He, Y. Niu and C. Yu, *Biosensors & bioelectronics*, 2015, 74, 953-959.
 30. X. Lu, Y. Li, X. Zhang, J. Du, X. Zhou, Z. Xue and X. Liu, *Analytica chimica acta*, 2012, 711, 40-45.
 31. C. I. Muller and C. Lambert, *Langmuir : the ACS journal of surfaces and colloids*, 2011, 27, 5029-5039.
 32. S. Xie, J. Zhang, Y. Yuan, Y. Chai and R. Yuan, *Chemical communications*, 2015, 51, 3387-3390.